

Contributions of different time scales to extreme Paraná floods

Andrés Antico¹ · María E. Torres^{1,2} · Henry F. Diaz³

Received: 11 December 2014 / Accepted: 14 August 2015
© Springer-Verlag Berlin Heidelberg 2015

Abstract The present study provides the first complete examination of how different time scales contributed to generate the four largest observed floods of the Paraná River (1905, 1983, 1992 and 1998). This inspection is based on the results from a previous study where an empirical method was used to decompose a 1904–2010 Paraná flow record (monthly means) into several physically meaningful oscillations with distinctive time scales or periods (few months to decades), and a secular increasing trend. We show that all the oscillations largely contributed to the four extreme floods, except an 18-year cycle that did not contribute to the 1992 flood. Sporadic intense constructive interferences between interannual-to-interdecadal (3–85 years) cycles determined (i) the favorable conditions for extreme-flood occurrence, and (ii) notable differences among floods. Indeed, in 1983, the largest flood ever recorded resulted mainly from an exceptionally strong constructive interference between cycles of 3–5, 9, 18 and 31–85 years, which are related to El Niño events, the North Atlantic Oscillation, the South Atlantic Convergence Zone, and the Pacific Ocean, respectively. Contributions

of the 31–85-year cycle to the two biggest floods (1983 and 1992) are larger than the contributions of the secular upward trend, suggesting the importance of this slow oscillation in flood formation processes. The implications of our results for understanding and predicting Paraná floods are discussed.

Keywords Paraná River · Extreme floods · Empirical time-scale decomposition · Climate oscillations

1 Introduction

The Paraná River has the third largest river discharge of South America (after the Amazon and Orinoco flows (Dai et al. 2009)) and is located in the southeastern part of this continent (Fig. 1). Occasionally (few times per century), the Paraná flow can be about two to three times greater than its climatological value, causing disastrous floods with high societal and economic impacts. For instance, the exceptionally severe Paraná flood of 1983 caused the evacuation of more than 200,000 people and economic losses of about one billion US dollars (Ministerio de Obras y Servicios Públicos 1984; Anderson et al. 1993). Because of these adverse consequences, several scientific studies had been undertaken to elucidate the climate forcings of extreme Paraná floods with the aim of providing valuable information for flood management (e.g., Camilloni and Barros 2000, 2003; Depetris 2007; Pasquini and Depetris 2010). Although these studies contributed notably to isolate and understand the role of some climate phenomena with specific time scales (e.g., El Niño events occurring every 3–7 years), there is still a need to perform a complete examination of all the different time scales and associated processes that are involved in the generation of massive Paraná floods

✉ Andrés Antico
aantico@santafe-conicet.gov.ar

¹ Consejo Nacional de Investigaciones Científicas y Técnicas, Facultad de Ingeniería y Ciencias Hídricas, Universidad Nacional de Litoral, Santa Fe, Santa Fe, Argentina

² Laboratorio de Señales y Dinámicas no Lineales, Facultad de Ingeniería, Universidad Nacional de Entre Ríos, Oro Verde, Entre Ríos, Argentina

³ National Oceanic and Atmospheric Administration, Earth System Research Laboratory, Cooperative Institute for Research in Environmental Sciences, University of Colorado, Boulder, CO, USA

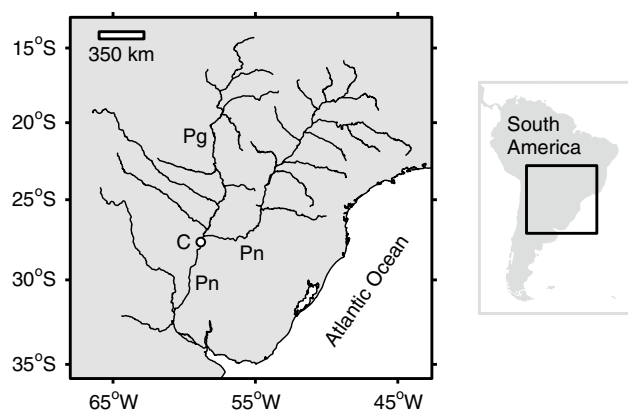


Fig. 1 Drainage system of the Paraná River. Two major rivers are labeled: Paraguay (Pg) and Paraná (Pn). The location of the Corrientes gauging station (C) is indicated by the open circle. It is noted that this station is downstream of the Pg and Pn confluence

(Camilloni and Barros 2003). Our objective here is to provide such an examination.

Recently, Antico et al. (2014, hereafter A14) significantly improved the characterization and description of Paraná flow changes with different time scales. They used a modern data-driven signal analysis method to fully decompose a 1904–2010 record of monthly Paraná flow into various oscillations with distinct time scales and a secular upward trend. In this study, we assess the contributions of these cycles and this trend to the Paraná discharge peaks of June 1905, June 1983, June 1992 and April 1998, which are the four most prominent peaks of the flow record considered in A14. That is, we break down each of these flood-flow peaks into the contributions (flow anomalies) corresponding to all the different time scales involved in the Paraná flow variability (these scales range from few months to several decades). Because different time scales are associated with different climate processes (see A14) and with different levels of forecastability, our results provide new and valuable insights into the causes and predictability of extreme Paraná floods.

2 Flow data and empirical methodology

The Paraná flow record used here and in A14 consists of monthly mean discharges at Corrientes gauging station (58° 50' W, 27° 29' S) for the interval January 1904–December 2010 (see station location in Fig. 1 and raw flow data in top of Fig. 2). We have verified that the main conclusions of this paper do not change if water levels at Corrientes station are used instead of discharges (results not shown). This is somehow expected since flow is calculated from water level through a rating curve.

Using the flow record presented above, we define extreme floods as the local flow maxima reaching or exceeding $4 \times 10^4 \text{ m}^3 \text{ s}^{-1}$ (roughly 2.5 times the climatological Paraná flow). Six flow maxima or peaks satisfy this condition: June 1905, December 1982, March 1983, June 1983, June 1992 and April 1998. It is noted, however, that the three peaks of 1982–1983 were part of the only high-flow ($>3 \times 10^4 \text{ m}^3 \text{ s}^{-1}$) time interval that lasted more than six months. To characterize this prolonged massive flood, we only consider its largest discharge peak (June 1983). Thus, henceforth we refer to the extreme Paraná floods as the flow peaks of June 1905, June 1983, June 1992 and April 1998 (peaks indicated in top of Fig. 2).

The Ensemble Empirical Mode Decomposition (EEMD) is a method designed to decompose nonlinear and nonstationary time series (like most hydroclimate records) into several oscillatory modes (Wu and Huang 2009; see a detailed EEMD description in “Appendix 1”). The characteristics of these modes (e.g., amplitude and frequency) are determined by the data itself and reflect the underlying driving processes. Although EEMD has already proved to be useful for analyzing geophysical data (Huang and Wu 2008), it also has some drawbacks that may limit the understanding of its results. For instance, the signal reconstructed by EEMD has a residual noise and the spectral separation of modes is not clear in most applications to real data. These limitations motivated Torres et al. (2011) to develop an improved variant of the EEMD method, named Complete EEMD with Adaptive Noise (CEEMDAN), that yields an exact reconstruction of the original time series and a clearer separation of modes (a detailed method description is given in “Appendix 2”). Because of these advantages, A14 used CEEMDAN to decompose the above-described Paraná flow record (denoted by Q) as follows: $Q = \sum_{k=1}^{10} Ck + R$, where Ck ($k = 1, \dots, 10$) are oscillatory modes (based on and derived from Q), and R is a residual secular upward trend. It must be stressed that (i) different modes Ck correspond to different time scales or oscillatory periods (i.e., A14 achieved a clear spectral separation of modes), and that (ii) the trend R encompasses all the time scales greater than the largest mode period. A14 successfully interpreted six oscillations or cycles, which are single modes or sums of modes, and the trend R (see our Fig. 2 for results of A14). In this study, values of these cycles and this trend for the times of extreme floods are considered as contributions of flow fluctuations with different time scales to these floods (see contributions in Figs. 2 and 3, and their associated time scales in Fig. 2). Because there is only one case of negative contribution (see Fig. 3), and for brevity, the term “contribution” is used hereafter to refer only to positive contributions.

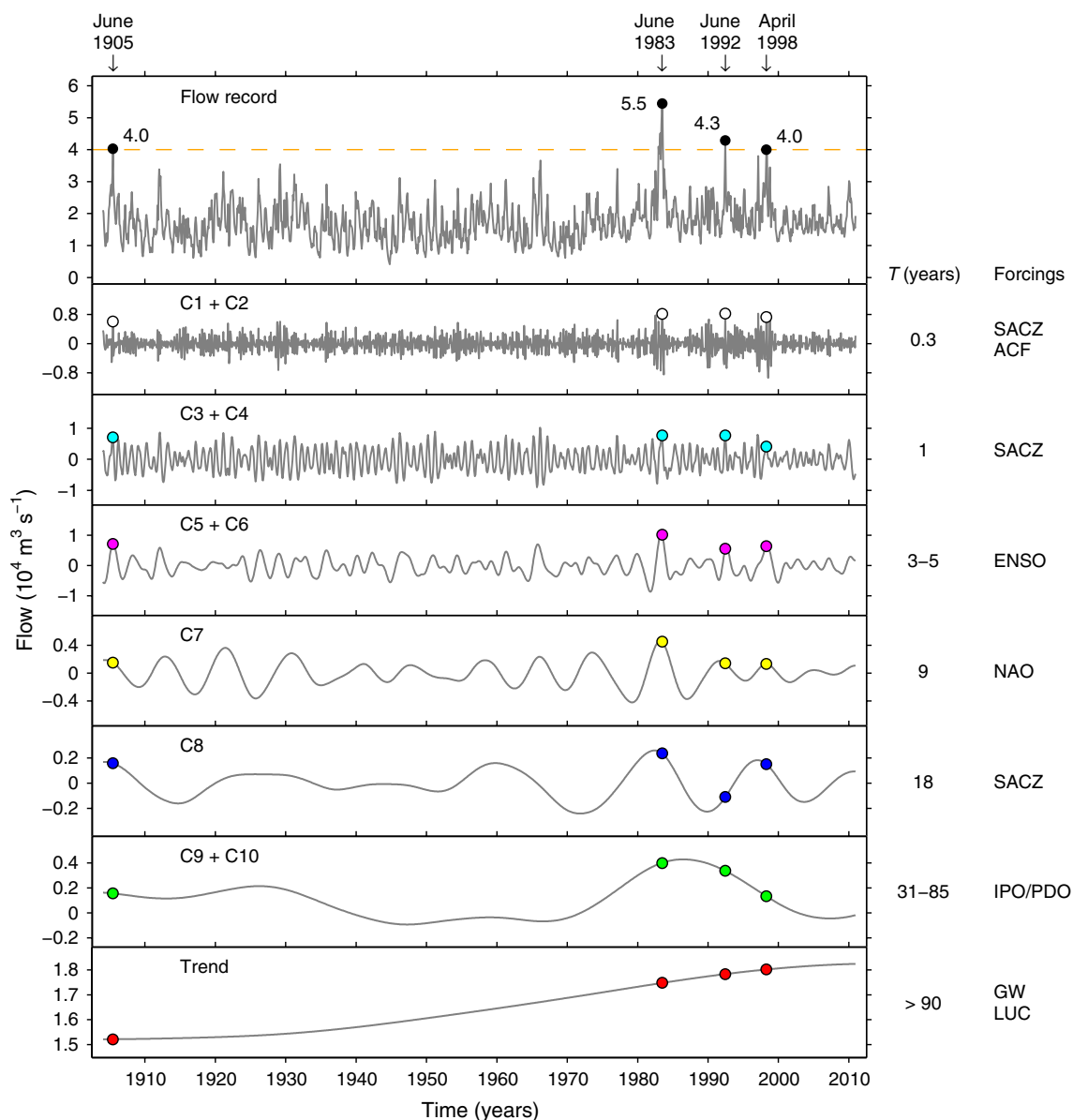


Fig. 2 Paraná flow record at Corrientes station, its oscillations, and its secular trend. Circles indicate the time series elements corresponding to June 1905, June 1983, June 1992 and April 1998, the times of extreme Paraná floods. In top, flows of these floods are given and the horizontal dashed line indicates the flow value of $4 \times 10^4 \text{ m}^3 \text{ s}^{-1}$, which is used to define extreme floods (see Sect. 2). Characteristic time scales (T) are shown and correspond to dominant oscillatory

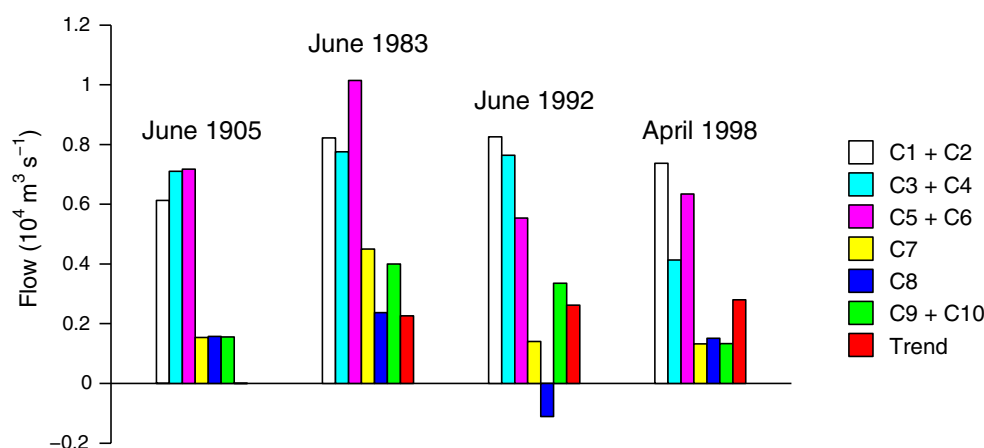
periods (see A14). Climate forcings are indicated (see A14 and text of this paper): South Atlantic Convergence Zone (SACZ), Atlantic cold fronts (ACF), El Niño/Southern Oscillation (ENSO), North Atlantic Oscillation (NAO), Interdecadal Pacific Oscillation/Pacific Decadal Oscillation (IPO/PDO), global warming (GW), and land use changes (LUC)

3 Results and discussion

Figure 3 reveals that all the flow oscillations contributed to generate all the extreme Paraná floods, except the 18-year cycle C8 that did not contribute to the 1992 flood. In most cases, the contributions resulted from the occurrence of cycle peaks at or near the times of the floods (Fig. 2). Nevertheless, it should be noted that other peaks of similar intensity occurred at other times when severe floods did not develop.

For instance, as shown in Fig. 2, the C7 peak associated with the 1983 extreme flood is similar to the C7 peak that occurred in the early 1920s, when extreme floods did not develop. Therefore, it is not possible to examine only one or two oscillations to explain the occurrences of extreme floods, and thus all (or most of) the cycles and the trend should be considered to understand these occurrences. Furthermore, as stated in the introduction, this consideration yields new insights into the causes and predictability of extreme floods

Fig. 3 Contributions of flow oscillations and trend to the extreme Paraná floods of 1905, 1983, 1992 and 1998. These contributions are depicted by *circles* in Fig. 2 (all panels except the *top panel*). The contributions of the secular upward trend are expressed as anomalies relative to January 1904 (start of the flow data interval)



because each oscillatory or trend change of flow is associated with a particular climate forcing (see a list of forcings in Fig. 2) and with a particular degree of forecastability. Consequently, in what follows we analyse how all (not few) the oscillations and the trend contributed to generate extreme Paraná floods, and discuss the implications of this analysis for understanding and predicting these severe events.

3.1 How do different cycles interfere to form extreme floods?

If, as mentioned above, all (or most of) the flow cycles should be taken into account to explain extreme floods, it is worth to here discuss how these oscillations act together to generate these floods. Figure 2 shows that all the extreme floods resulted from unusual additions of time-aligned large peaks of all or most flow cycles, i.e., six or five cycles. More specifically, total or partial alignments of six large peaks led to the extreme floods of 1905, 1983 and 1998, and a near alignment of five large peaks led to the extreme flood of 1992 (see Fig. 2). It is also observed in Fig. 2 that although other alignments of six or five peaks occurred at other times, they did not result in extreme floods because some of the involved peaks were not strong enough to guarantee the formation of such floods. Note for instance in Fig. 2 that the six-peak alignments observed in the early 1920s did not generate extreme floods because the small amplitude of some peaks (e.g., peaks of C5 + C6 and C8) precluded strong constructive interferences between all the six cycles. Hence, our results suggest that extreme floods reflect infrequent and exceptionally intense constructive interferences between large (not small) peaks of all or most flow cycles.

3.2 The importance of interannual and interdecadal cycles in extreme-flood formation

Although we have shown in previous section that the generation of extreme Paraná floods involves many flow

cycles (i.e., many time scales), we have not yet analyzed the relative importances of different cycles in promoting these floods. In this regard and as it will be discussed later (Sect. 3.6), it is of practical relevance to analyze the importance of interannual-to-interdecadal cycles. Thus, this analysis is conducted below in this section.

Figure 4 shows that interannual and longer cycles exerted an important control on the development of large flows because outstanding peaks of the raw flow record tend to coincide with prominent peaks of the sum of interannual and interdecadal flow oscillations (C5 + C6, C7, C8 and C9 + C10). In fact, the four highest peaks of this sum coincide with the four most severe floods (1905, 1983, 1992 and 1998; see Fig. 4), referred here as extreme floods (see Sect. 2). From this result and the discussion presented in previous section, it is evident that the favourable conditions for extreme-flood formation were largely set by sporadic strong constructive interferences between interannual and longer discharge cycles. These interferences also explain the large discrepancies observed between the intensities of different extreme floods, which can not be explained by only looking at the intraannual and annual cycles (C1 + C2 and C3 + C4, respectively). Note, for example, that while the large difference between the 1983 and 1992 floods can be explained by the sum of interannual and longer cycles (see black curve in Fig. 4), it can not be explained in terms of changes in C1 + C2 and C3 + C4 because C1 + C2 contributed almost equally to these two floods, and the same situation is observed for C3 + C4 (see Figs. 2 and 3). Consequently, given the importance of interannual-to-interdecadal cycles in generating and shaping extreme floods, the remaining discussions will be focused on these cycles.

3.3 Why was the 1983 flood so extreme?

As observed in Fig. 2 (top), the 1983 flood was by far larger than other extreme floods. Given that large differences between extreme floods were mainly created by interannual

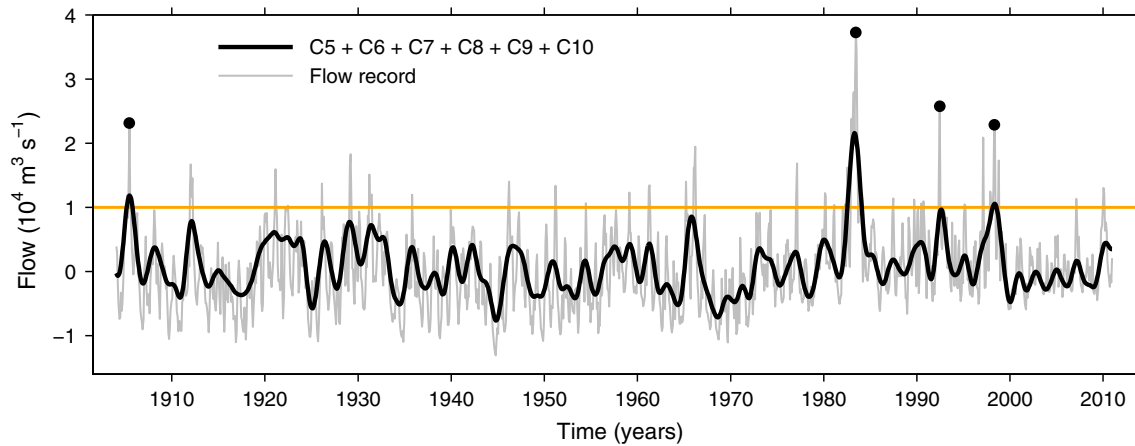


Fig. 4 Paraná flow record (same of *top* of Fig. 2 but with its mean subtracted) and the sum of the interannual-to-interdecadal flow cycles C5 + C6, C7, C8 and C9 + C10 (thick *black curve*; see individual

cycles in Fig. 2). The *horizontal line* ($+10^4 \text{ m}^3 \text{ s}^{-1}$) is shown to facilitate the visual comparison of different peaks. *Circles* indicate the extreme floods of 1905, 1983, 1992 and 1998

and interdecadal flow cycles (see previous section), these cycles are considered below to explain the exceptional intensity of the 1983 flood.

Remarkably, the interannual-to-interdecadal cycles C5 + C6, C7, C8 and C9 + C10 contributed more to the 1983 flood than to the other extreme floods (see Fig. 3) because the largest peaks of all these cycles occurred approximately synchronously around 1983 (Fig. 2). As revealed in Fig. 4, these aligned strong peaks added constructively in 1983 to generate an exceptionally large flow peak that had no analogue in the remaining years of the interval 1904–2010. It is then clear that this one-in-a-century constructive interference between C5 + C6, C7, C8 and C9 + C10 is the main reason to explain the extraordinary severity of the 1983 flood. Thus, our results suggest that an unusually strong additive effect of the climate forcings of these cycles may have played an important role in the generation of the massive 1983 flood. These forcings are listed in Fig. 2 and discussed in the next section.

3.4 Contributions of interannual and interdecadal cycles (C5–10) to extreme floods: roles of different climate forcings

Large local maxima of the 3–5 year cycle C5 + C6 occurred at the times of all extreme floods (Fig. 2), and hence this flow oscillation contributed to these floods (Fig. 3). Since prominent peaks of C5 + C6 tend to coincide with El Niño events (see Fig. 6 of A14), our results are consistent with previous studies where a relation between El Niño episodes and large Paraná floods was elucidated (e.g., Camilloni and Barros 2000, 2003). During El Niño years, an intensification of the subtropical jet stream enhances the baroclinic activity and associated rainfall

over the Paraná Basin (see Garreaud et al. 2009, and references therein).

Observational studies revealed a relation between an 8–9-year Paraná flow cycle, described here by C7, and a similar cycle of the North Atlantic Oscillation (NAO) (Robertson and Mechoso 1998; Nogués-Paegle et al. 2000; Labat et al. 2005; A14). Using climate reanalyses, Nogués-Paegle et al. (2000) found that during positive (negative) states of the decadal NAO cycle, an intensification (weakening) of the trade winds in the tropical North Atlantic Ocean enhances (diminishes) the moisture advection from this ocean to South America and this, in turn, increases (decreases) precipitation and river flow in the Paraná basin. This explains why the flow peaks of the 9-year cycle C7 nearly coincided with positive states of the decadal NAO cycle (see Fig. 7 of A14). Therefore, considering this and that all extreme Paraná floods received contributions from C7 peaks (see Figs. 2 and 3), we propose that such floods may be more likely to occur when the decadal NAO cycle is in a positive state. It is noticed that, besides the NAO forcing of C7, a solar influence on C7 was proposed (Antico and Kröhling 2011). However, since this Sun-Paraná flow link remains speculative, its role in flood formation is not discussed here.

The 18-year cycle C8 appears to be driven by changes in the the South Atlantic Convergence Zone (SACZ), which are related to an anomalous upper-tropospheric large-scale eddy located in the lee side of the Andes Mountains (Robertson and Mechoso 2000). Given that C8 contributed to three of the four extreme floods (1905, 1983 and 1998; see Fig. 3), the bidecadal SACZ variability seems to be an important climate factor for the generation of massive Paraná floods.

Interdecadal Paraná flow changes like those reflected by the 31–85-year cycle C9 + C10 are linked to the

Interdecadal Pacific Oscillation (IPO), also known as the Pacific Decadal Oscillation (PDO), in a manner that positive (negative) states of the IPO/PDO cause positive (negative) anomalies of flow (Dettinger and Diaz 2000; Dettinger et al. 2001; A14). Because of this, and since all the extreme floods occurred only when C9 + C10 had positive flow anomalies (i.e., C9 + C10 contributed to these floods; see Figs. 2 and 3), we suggest that extreme Paraná floods are more prone to develop during positive (El Niño-like) IPO/PDO states.

3.5 Pacific-related interdecadal cycle versus the secular trend

Interestingly, the two most extreme floods (1983 and 1992) occurred at the top of the largest peak of the Pacific-related interdecadal cycle C9 + C10 (see Fig. 2). As a result, the contributions of C9 + C10 to these two floods were larger than the secular trend increase in flow from the mid 1900s to the early 1990s (Fig. 3). This suggests that the role of the IPO/PDO (Pacific forcing of C9 + C10; see above) in extreme-flood formation would be more important than the role of the possible drivers of the secular upward trend of flow, which are global warming and land use changes (these trend drivers are discussed in A14). To further suggest this important IPO/PDO role, it is noted that the absence of extreme floods after 2000 (see top of Fig. 2) is consistent with the apparent early-2000s transition of the IPO/PDO from a positive to a negative state (Lee and McPhaden 2008; Cai and van Rensch 2012) since, as discussed in previous section, this transition would reduce the likelihood of extreme floods.

3.6 Prospects for predicting the risk of extreme floods

Successful data-based climate predictions can be achieved if the predictable part of data is isolated prior to prediction. Salisbury and Wimbush (2002), and Wu (2008) showed that the Empirical Mode Decomposition (EMD) method and its variants (e.g., EEMD and CEEMDAN) can be used to separate the predictable slow (interannual and longer) oscillations from the unpredictable or hardly predictable fast (annual or shorter) changes. These authors obtained promising forecasts of El Niño and La Niña events by first isolating (with EMD or EEMD) and then forecasting the interannual-to-interdecadal predictable cycles of El Niño index records; while Wu (2008) obtained a 1-year prediction that is based on the forecasts of several individual EMD cycles, Salisbury and Wimbush (2002) used one interannual EEMD cycle to perform a 4-year prediction. We speculate that similar procedures can be used to predict the sum of the interannual-to-interdecadal CEEMDAN oscillations of Paraná flow, which we

believe are predictable for at least one year. Since this sum of slow cycles (black line in Fig. 4) largely determines whether extreme Paraná floods occur or not (see Sect. 3.2), its potential empirical predictability implies that it would be possible to anticipate years with high or low risk of extreme floods. Certainly, achieving this anticipation will improve hazard management in the Paraná basin; we leave this possible task for future studies.

4 Conclusions

We have examined the contributions of different time scales to the four biggest floods observed in the Paraná River (1905, 1983, 1992 and 1998). These contributions are derived from the results of a previous study where a 1904–2010 Paraná flow record was empirically decomposed into six physically meaningful oscillations with different time scales or periods (few months to decades), and a secular upward trend. The main conclusions of this work are:

- All the flow oscillations contributed to form the four considered extreme floods, except a bidecadal cycle that did not contribute to the 1992 flood. This not only confirms previously obtained results (e.g., a link between large floods and El Niño events), but it also reveals new ones like a possible relation between extreme Paraná floods and positive states of a decadal cycle of the North Atlantic Oscillation.
- Extreme floods are created by sporadic intense constructive interferences between all (or most of) the flow cycles. Nevertheless, only the interannual and interdecadal oscillations played an important role in (i) determining the favourable conditions for massive-flood formation, and in (ii) creating marked differences between flood intensities. This implies that years with high risk of extreme floods may be anticipated because interannual and longer cycles could be predictable.
- The 1983 flood was by far the largest ever recorded, and this mainly resulted from an unusually intense constructive interference between flow cycles of 3–5, 9, 18, and 31–85 years, which are driven by different (known) climate forcings (listed in Fig. 2 of this paper). To our knowledge, our study is the first to report the key role of this interference in the generation of the 1983 Paraná flood.
- The contributions of a 31–85-year flow cycle to the two largest floods (1983 and 1992) are greater than the contributions of the secular upward trend of flow. This suggests that the interdecadal Pacific variability, forcing of the 31–85-year cycle, may exert an appreciable long-term control on the probability of extreme Paraná floods.

As a final note, we mention that our original empirical approach yields an improved understanding of Paraná floods that constitutes a valuable basis for future numerical and observational studies of these natural disasters.

Acknowledgments We are grateful to two anonymous reviewers for their constructive comments that greatly improved the manuscript. Paraná flow data were provided by the Subsecretaría de Recursos Hídricos, Argentina (data available at <http://www.hidricosargentina.gov.ar>). This research was supported by the Universidad Nacional del Litoral through the CAI+D and PIRHCa programs.

Appendix 1: EEMD method

The Empirical Mode Decomposition (EMD) is a data-driven method that was proposed to decompose nonlinear and nonstationary time series into oscillatory modes called Intrinsic Mode Functions (IMFs) (Huang et al. 1998). An IMF is defined as a signal or time series that satisfies two conditions: (i) the number of extrema and the number of zero crossings must be either equal or differ at most by one, and (ii) the mean value of the upper and lower envelopes is zero at any point. In the Ensemble EMD (EEMD), definitive modes are defined as the average of the IMFs obtained through EMD over an ensemble of trials, generated by adding different white noise realizations to the original time series x (Wu and Huang 2009). More precisely, the EEMD algorithm is described as follows:

1. generate $x^i = x + w^i$, where w^i ($i = 1, \dots, I$) are different realizations of white Gaussian noise of specified variance;
2. use EMD to fully decompose each x^i into the modes IMF_k^i , where $k = 1, \dots, K$ indicates the mode number;
3. assign \overline{IMF}_k as the k -th mode of x , obtained as the average of the corresponding EMD modes: $\overline{IMF}_k = \frac{1}{I} \sum_{i=1}^I IMF_k^i$.

Appendix 2: Complete EEMD with Adaptive Noise

In EEMD, each x^i is decomposed independently from the other realizations (see “Appendix 1”). Therefore, different realizations lead to different residues $r_k^i = r_{k-1}^i - IMF_k^i$, where $r_0^i = x^i$. In the Complete EEMD with Adaptive Noise (CEEMDAN), where the definitive k -th mode is notated as \widetilde{IMF}_k , a single first residue is obtained as $r_1 = x - \widetilde{IMF}_1$, with \widetilde{IMF}_1 being the first EEMD mode (Torres et al. 2011). Then, the first EMD mode is computed over an ensemble of r_1 plus different realizations of a given noise, and \widetilde{IMF}_2 is obtained by averaging. The procedure continues with the rest of modes until a stopping criterion is attained.

Defining the operator $E_j(\cdot)$, which gives the j -th mode obtained by EMD, and letting w^i be zero-mean unit-variance white Gaussian noise, the CEEMDAN algorithm can be described as follows:

1. perform an EMD decomposition of I realizations $x + \beta_0 w^i$ (hereafter the letter β is used for coefficients) and use the obtained first modes to compute:

$$\widetilde{IMF}_1 = \frac{1}{I} \sum_{i=1}^I IMF_1^i = \overline{IMF}_1;$$

2. calculate the first residue as: $r_1 = x - \widetilde{IMF}_1$;
3. find the first EMD modes of the realizations $r_1 + \beta_1 E_1(w^i)$ and define the second mode as:

$$\widetilde{IMF}_2 = \frac{1}{I} \sum_{i=1}^I E_1(r_1 + \beta_1 E_1(w^i));$$

4. for $k = 2, \dots, K$ calculate the k -th residue as: $r_k = r_{(k-1)} - \widetilde{IMF}_k$;
5. obtain the first EMD modes of the realizations $r_k + \beta_k E_k(w^i)$ and define the $(k + 1)$ -th mode as:

$$\widetilde{IMF}_{(k+1)} = \frac{1}{I} \sum_{i=1}^I E_1(r_k + \beta_k E_k(w^i));$$

6. go to step 4 for next k .

Observe in steps 1–5 that the levels of added noise are determined by the coefficients β_k . Steps 4–6 are performed until the obtained residue can no longer be decomposed (i.e., the residue does not have at least two extrema). This leads to a residual trend R that satisfies:

$$R = x - \sum_{k=1}^K \widetilde{IMF}_k.$$

For the sake of simplicity, the k -th mode \widetilde{IMF}_k is notated as C_k in this study.

References

- Anderson RJ, da Franca Ribeiro dos Santos N, Diaz HF (1993) An Analysis of Flooding in the Paraná/Paraguay River Basin. LATEN Dissemination Note No. 5, The World Bank, Washington, DC
- Antico A, Kröhling DM (2011) Solar motion and discharge of Paraná River, South America: evidence for a link. *Geophys Res Lett* 38: doi:10.1029/2011GL048851
- Antico A, Schlotthauer G, Torres ME (2014) Analysis of hydro-climatic variability and trends using a novel empirical mode decomposition: application to the Paraná River Basin. *J Geophys Res Atmos* 119:1218–1233. doi:10.1002/2013JD020420

- Cai W, van Rensch P (2012) The 2011 southeast Queensland extreme summer rainfall: a confirmation of a negative Pacific Decadal Oscillation phase? *Geophys Res Lett* 39: doi:[10.1029/2011GL050820](https://doi.org/10.1029/2011GL050820)
- Camilloni IA, Barros VR (2000) The Paraná River response to El Niño 1982–83 and 1997–98 events. *J Hydrometeorol* 1:412–430
- Camilloni IA, Barros VR (2003) Extreme discharge events in the Paraná River and their climate forcing. *J Hydrol* 278:94–106
- Dai A, Qian T, Trenberth KE, Milliman JD (2009) Changes in continental freshwater discharge from 1948 to 2004. *J Clim* 22:2773–2792. doi:[10.1175/2008JCLI2592.1](https://doi.org/10.1175/2008JCLI2592.1)
- Depetris PJ (2007) The Parana river under extreme flooding: a hydrological and hydro-geochemical insight. *Interciencia* 32:656–662
- Dettinger MD, Diaz HF (2000) Global characteristics of stream flow seasonality and variability. *J Hydrometeorol* 1:289–310
- Dettinger MD, Battisti DS, Garreaud RD, McCabe GJ, Bitz CM (2001) Interhemispheric effects of interannual and decadal ENSO-like climate variations on the Americas. In: Markgraf V (ed) *Interhemispheric climate linkages: present and past climates in the Americas and their societal effects*. Academic Press, London, pp 1–16
- Garreaud RD, Vuille M, Compagnucci R, Marengo J (2009) Present-day South American climate. *Paleog Paleoclim Paleoecol* 281:180–195. doi:[10.1016/j.palaeo.2007.10.032](https://doi.org/10.1016/j.palaeo.2007.10.032)
- Huang NE, Wu Z (2008) A review on Hilbert-Huang transform: method and its applications to geophysical studies. *Rev Geophys* 46:8755–1209. doi:[10.1029/2007RG000228](https://doi.org/10.1029/2007RG000228)
- Huang NE, Shen Z, Long SR, Wu MC, Shih HH, Zheng Q, Yen NC, Tung CC, Liu HH (1998) The empirical mode decomposition and the Hilbert spectrum for nonlinear and non-stationary time series analysis. *Proc R Soc London Ser A* 454:903–995
- Labat D, Ronchail J, Guyot JL (2005) Recent advances in wavelet analyses: part 2—Amazon, Parana, Orinoco and Congo discharges time scale variability. *J Hydrol* 314:289–311. doi:[10.1016/j.jhydrol.2005.04.004](https://doi.org/10.1016/j.jhydrol.2005.04.004)
- Lee T, McPhaden MJ (2008) Decadal phase change in large-scale sea level and winds in the Indo-Pacific region at the end of the 20th century. *Geophys Res Lett* 35: doi:[10.1029/2007GL032419](https://doi.org/10.1029/2007GL032419)
- Ministerio de Obras y Servicios Públicos (1984) Informe de daños. Crecida 1982–83 de los ríos Paraná, Paraguay y Uruguay. Buenos Aires, Argentina
- Nogués-Paegle J, Robertson AW, Mechoso CR (2000) Relationship between the North Atlantic Oscillation and river flow regimes of South America. In: *Proceedings of the 25th annual climate diagnostics and prediction workshop*. Palisades, NY, pp 323–326
- Pasquini AI, Depetris PJ (2010) ENSO-triggered exceptional flooding in the Paraná River: where is the excess water coming from? *J Hydrol* 383:186–193. doi:[10.1016/j.jhydrol.2009.12.035](https://doi.org/10.1016/j.jhydrol.2009.12.035)
- Robertson AW, Mechoso CR (1998) Interannual and decadal cycles in river flows of southeastern South America. *J Clim* 11:2570–2581
- Robertson AW, Mechoso CR (2000) Interannual and interdecadal variability of the South Atlantic convergence zone. *Mon Wea Rev* 128:2947–2957
- Salisbury JI, Wimbush M (2002) Using modern time series analysis techniques to predict ENSO events from the SOI time series. *Nonlin Process Geophys* 9:341–345. doi:[10.5194/npg-9-341-2002](https://doi.org/10.5194/npg-9-341-2002)
- Torres ME, Colominas MA, Schlotthauer G, Flandrin P (2011) A complete ensemble empirical mode decomposition with adaptive noise. In: *IEEE international conference on acoustics, speech and signal processing*. ICASSP-11, Prague (CZ), pp 4144–4147. doi:[10.1109/ICASSP.2011.5947265](https://doi.org/10.1109/ICASSP.2011.5947265)
- Wu Z (2008) Annual cycle and prediction of interannual variability. *Climate Test Bed Joint Seminar Series*. US National Oceanic and Atmospheric Administration, Maryland
- Wu Z, Huang NE (2009) Ensemble empirical mode decomposition: a noise-assisted data analysis method. *Adv Adapt Data Anal* 1:1–41. doi:[10.1142/S1793536909000047](https://doi.org/10.1142/S1793536909000047)